Variety in intracellular diffusion during the cell cycle

2009 Phys. Biol. 6 025015

(http://iopscience.iop.org/1478-3975/6/2/025015)

Phys. Biol. **6** (2009) 025015 (9pp) doi:10.1088/1478-3975/6/2/025015

Variety in intracellular diffusion during the cell cycle

Christine Selhuber-Unkel[1], Pernille Yde[1], Kirstine Berg-Sørensen[2] and Lene B Oddershede[1]

[1] The Niels Bohr Institute, University of Copenhagen, Blegdamsvej 17, 2100 Copenhagen, Denmark
[2] Department of Physics, Danish Technical University, 2800 Kgs. Lyngby, Denmark

E-mail: oddershede@nbi.dk

Received 29 August 2008
Accepted for publication 17 November 2008
Published 1 July 2009
Online at stacks.iop.org/PhysBio/6/025015

Abstract
During the cell cycle, the organization of the cytoskeletal network undergoes dramatic changes. In order to reveal possible changes of the viscoelastic properties in the intracellular space during the cell cycle we investigated the diffusion of endogenous lipid granules within the fission yeast *Schizosaccharomyces Pombe* using optical tweezers. The cell cycle was divided into interphase and mitotic cell division, and the mitotic cell division was further subdivided in its stages. During all stages of the cell cycle, the granules predominantly underwent subdiffusive motion, characterized by an exponent α that is also linked to the viscoelastic moduli of the cytoplasm. The exponent α was significantly smaller during interphase than during any stage of the mitotic cell division, signifying that the cytoplasm was more elastic during interphase than during division. We found no significant differences in the subdiffusive exponents from granules measured in different stages of cell division. Also, our results for the exponent displayed no significant dependence on the position of the granule within the cell. The observation that the cytoplasm is more elastic during interphase than during mitotic cell division is consistent with the fact that elastic cytoskeletal elements such as microtubules are less abundantly present during cell division than during interphase.

1. Introduction

Cell division is the essential mechanism that regulates the reproduction and growth of all organisms. During cell division, the cytoskeletal microtubules and actin filaments act in a concerted fashion in order to separate the two daughter chromosomes and generate two daughter cells. There are two types of cell division: meiotic and mitotic cell division, which refer to sexual and asexual cell division, respectively. In contrast to the meiotic cell division, mitotic cell division only involves a single mother cell, from which two daughter cells are generated. Mitosis always starts with the replication of the chromatids in the nucleus. Subsequently, an organized network of microtubule polymers forms, known as the *mitotic spindle*. During mitosis, the mitotic spindle attaches to the replicated chromatids from the cell nucleus and provides the mechanical framework for the separation of the daughter chromatids. This step is essential for the later *cytokinesis*, where the two daughter cells are separated [1].

A popular eucaryotic cell for studying cell cycle, morphology and control pathways is the fission yeast *Schizosaccharomyces pombe* (*S. pombe*). It is frequently used because it is relatively easy to genetically modify and its cell division mechanism resembles to a large extent that of higher cells [2, 3]. In contrast to most other cells, the mitotic spindle in *S. pombe* is formed inside the nucleus, not outside. Schematic drawings of the different stages in *S. pombe* mitosis (and cytokinesis) are shown in figure 1. To take the fluorescent images we used an *S. pombe* yeast strain which had been genetically modified such that the lipids in the nuclear and plasma membranes were fluorescently marked with green fluorescent protein. In particular, the nuclear membrane is clearly visible in this strain. A *S. pombe* cell spends most of its life time in interphase. When an *S. pombe* cell starts to divide (prophase), the intranuclear spindle forms once the spindle pole body, a microtubule-organizing center, has duplicated and separated. The actin filaments are in this stage located around the nucleus and cytoplasmic microtubules have disappeared,

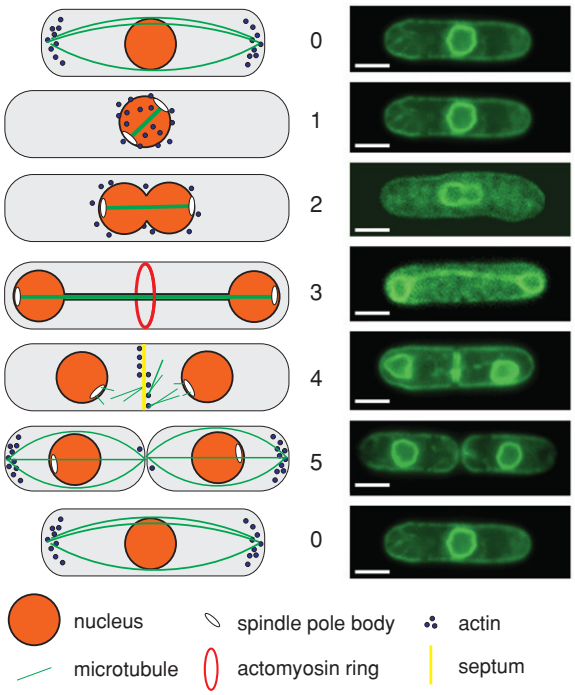

Figure 1. Sketch of the *S. Pombe* life cycle stages (left). (0) The cell spends most of its time in interphase where bundled long microtubules (green) span the cytoplasm and assist in keeping the nucleus centered, actin patches (dots) accumulate at the ends of the cell. (1) An early mitotic cell, where an intranuclear spindle made of microtubules has formed. The actin surrounds the nucleus and no microtubules are present in the cytoplasm. (2) A cell in early anaphase, where the spindle pushes the two ends of the nucleus apart. (3) Mitosis is further progressing, the spindle has just finished elongating and pushed the two daughter nuclei to the ends of the cell. In the middle of the cell, an actomyosin ring has formed; this stage is denoted late anaphase or early telophase. (4) A cell at the end of mitosis (early cytokinesis), where the mitotic spindle has disappeared, and a septum (yellow) appears while the actomyosin ring is getting ready to contract. (5) Cytokinesis is finished and two daughter cells have formed. Actin is relocated to the ends of the cell and cytoplasmic microtubules reappear. Fluorescence images of the *S. pombe* cells in their different life cycle stages in our experiments (right). The cellular membrane systems are marked with green fluorescent protein. Scale bar: 5 μm.

also, the cell starts to elongate. Next (early anaphase), the spindle elongates inside the nucleus where it pushes at the two extremes of the mother nucleus, allowing for transformation into two daughter nuclei. As soon as the daughter nuclei have separated, they are relocated toward the two ends of the cell by the spindle microtubules (late anaphase). The telophase begins when the two daughter nuclei stop migrating toward the ends of the mother cell. An actomyosin ring appears in the middle of the cell. This ring contracts and induces the formation of a septum, which finally separates the two daughter cells (cytokinesis) [2, 4]. Hence, large parts of the cell cytoskeleton and cytoplasm are rearranged during mitosis and this motivated our investigation of possible changes in cytoplasmic viscoelasticity during the cell cycle.

It was shown by Mason and Weitz [5] that a probe particle can be used to measure viscoelasticity of a bulk complex fluid by dynamic light scattering. Fluorescence correlation spectroscopy is an alternative method to measure diffusion of molecules in viscoelastic media, this method requiring a fluorescent marker on the molecule of interest [6]. Often, video based multiple particle tracking or laser tracking microrheology is used to study the motion of non-fluorescent probes embedded in viscoelastic media. Multiple particle tracking uses fast video cameras to optically follow the position of particles and subsequent video analysis provides a positional precision in the detection down to tens of nanometers. This method has successfully been applied in living cells [7, 8], but also in biomimetic systems [9]. In laser tracking microrheology, the position detection system of optical tweezers is used to track the motion of colloidal particles with nanometer precision using comparably small laser powers [10–12]. Whereas optical tweezers are capable of studying diffusion at short timescales, optical particle tracking is typically used for studying diffusion and transport processes at larger timescales (>0.01 s) and a combination of these methods yields quite a large frequency range [13].

Many biomimetic experiments studying the viscoelastic properties and microrheology of networks and gels of cytoskeletal elements have been performed. Such studies have shown that particles in gels of semi-flexible actin networks perform subdiffusion [14, 15] and that the rheological properties of actin networks are highly dependent on the confinement of the network and on single-filament fluctuations [16]. Furthermore, it has been proven that adding motor proteins to actin solutions changes the viscoelastic properties and stiffness of the network [17].

In recent years, *in vivo* studies of the viscoelastic properties of the intracellular space have attracted more and more interest. In many experiments, the diffusion of endogenous lipid granules is studied [8, 13, 18]. One big advantage of the lipid granules is that they occur naturally and are therefore not regarded as foreign objects by the cell, whereas non-endogenous particles can induce active intracellular transport processes [19]. The different types of diffusive motion of a probe particle in a complex medium can be distinguished through the rheological exponent, α. The mean squared displacement of the probe particle, $\langle \Delta x(t)^2 \rangle$, is a function of time, t, and given as $\langle \Delta x(t)^2 \rangle = 2Dt^{\alpha}$, where D is the diffusion constant. If $\alpha < 1$ the motion is termed subdiffusive, if α=1 it is a normal diffusive motion in a purely viscous medium, and if $\alpha > 1$ the motion is superdiffusive. Earlier work on the diffusion of lipid granules in interphase *S. pombe* cells using optical tweezers and multiple-particle tracking showed that different types of diffusion can be detected in the intracellular space, with a rheological exponent, α, that depends on the timescale in question: on timescales shorter than 10^{-3} s, only subdiffusion was observed. For timescales longer than 10^{-1} s, also other types of motion have been detected, e.g., confined motion, normal Brownian motion and superdiffusive motion [13, 18]. All these types of motion were interpreted as indicative of specific biological processes in the cell.

In the present study we focused on the diffusion of intracellular granules in *S. pombe* cells at short timescales with the goal of investigating whether and how the viscoelasticity

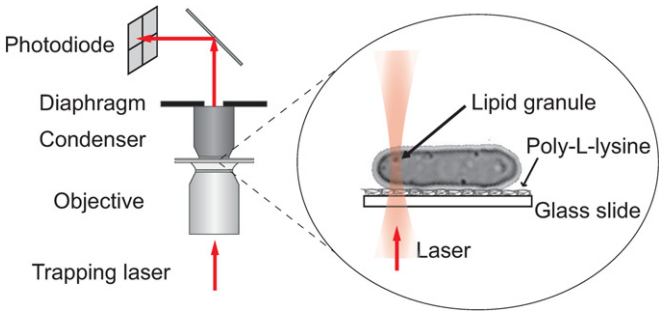

Figure 2. Illustration of the optical tweezers setup used for the experiments. The cell is attached to the lower glass slide of the perfusion chamber with poly-L-lysine. The position of a lipid granule is tracked by recording the forward-scattered laser light with a quadrant photodiode.

of the cell cytoplasm changes during the cell division cycle. The position of the endogenous lipid granules was tracked by optical tweezers with nanometer resolution. The positional information of the granules was analyzed using a power spectral analysis method for optical tweezers data, which also corrected for parasitic filtering by the data acquisition system. Our results showed that the granules underwent subdiffusion in the cellular cytoplasm in all phases of the cell cycle. When the cells were in interphase the subdiffusive exponent was 0.81 which is close to that found for semi-flexible polymer solutions. In all stages of mitosis (and cytokinesis) we found the subdiffusive exponent to be significantly larger than in interphase, but with no observable difference between the various stages of cell division. We also investigated whether the position of the granule relative to the cell nucleus was significant for the observed viscoelasticity in the surrounding cytoplasm: by comparing the subdiffusive exponents from granules stemming from different spatial zones of the cell we found no significant difference between granules located between or outside the two daughter nuclei of cells in anaphase. Also, we did not see any relation between the subdiffusive exponent and distance to cell nucleus for interphase cells.

2. Materials and methods

2.1. Cell sample preparation

We used *S. pombe* cells (D817) that were expressing a GFP-fused marker of the nuclear and plasma membrane systems [20]. When the cells are in interphase, they have a length of approximately 12 μm and a width of about 4 μm. Spherical lipid granules, about 300 nm in diameter, occur naturally in the cytoplasm of the cells [21]. These granules are highly refractive so that they are visible in a light microscope (figure 2) and can be tracked with the optical tweezers. They are ideal particles for intracellular diffusion studies, as the stiff cell wall of the fission yeast does not allow an easy incorporation of extracellular particles into its intracellular space. The cells were cultured on AA-Leu agar plates for 12–14 h at 30 °C and afterward stored at 4 °C. Prior to the experiments, the cells were diluted and grown in liquid AA-Leu medium over night at 30 °C in a shaking water bath. This treatment ensured that the cells underwent mitotic and not meiotic cell division.

The fluid chamber for the experiments consisted of two glass slides glued together by two layers of double sticky tape as a spacer. In order to make the cells stick to the bottom of the fluid chamber, its surface was coated with a thin layer of Poly-L-Lysine (Sigma, P8920) by spreading it on the glass surface and letting it dry. The chamber was filled with AA-Leu medium before the cell suspension was added. In order to let the cells establish a firm contact with the surface, they were left to stick to the surface for 15–20 min prior to the experiments.

2.2. Optical measurements

Optical tweezers were formed using a Nd:YVO_4 laser (5W Spectra Physics BL-106C, $\lambda = 1064$ nm, TEM_{00}), which was implemented in an inverted fluorescence microscope (Leica, DMI 6000) equipped with a cooled CCD camera (Andor, Ixon cooled EMCCD). In the experiments we used an oil immersion objective from Leica (HCX PL Apo, $100\times/\mathrm{NA} = 1.4$ oil Cs). The forward scattered light of the highly-refractive intracellular granules was recorded using a silicon quadrant photodiode (S5981, Hamamatsu) in the back focal plane, which measures the position of the granule in the laser focus with nanometer precision. Figure 2 shows a sketch of our experimental setup. In an experiment, the motion of a single granule in the laser focus was tracked for approximately 3 s at a sampling frequency of 22 kHz. We used a laser power of approximately 0.05 W at the sample. The voltage signal from the photodiode was digitalized using home-written Labview algorithms. All experiments were done at room temperature, 22–23 °C.

When performing optical tweezers experiments on biological specimen one should be cautious about possible damage in the specimen caused by the trapping laser light. It is well known that optical tweezers with wavelengths in the infra-red cause less damage than visible lasers. In [22] the physiological state of an optically trapped bacterium was monitored by its ability to obtain a pH gradient across its cell wall. This study showed that if a 1064 nm laser is used, if the exposure powers are similar to those used in the present study, and if exposure time is less than 10 min, no physiological damage is detectable. Another recent study shows that comprised ability to express green fluorescent protein is related to the total dose delivered by the laser [23]. In the present study we are far below any threshold where physiological damage has ever been reported on optically trapped specimen. Also, the heating of the specimen with the laser powers used is less than 1 °C [24].

The cells were illuminated by a Hg lamp and imaged by the cooled CCD camera. Just before and after the optical tweezers data were acquired, the Hg lamp was off and the cell filmed by bright-field illumination where the trapped granule was clearly visible. This procedure ensured that we kept track of the position of the trapped granules with respect to the cell and that we were able to determine the status of the cell within its life cycle.

2.3. Data analysis

The equation of motion for a freely diffusing particle in a viscous fluid in one dimension, x, is given by

$$m\ddot{x}(t) = -\gamma\dot{x}(t) + F(t), \tag{1}$$

where m is the mass of the particle and $-\gamma\dot{x}(t)$ represents the drag force on the particle. $F(t)$ is a thermal noise term, which is caused by random collisions of the particle with surrounding molecules. To further analyze the motion of the diffusing particle, the equation of motion can be Fourier transformed and the resulting power spectrum is

$$\langle|\tilde{x}(f)|^2\rangle = \frac{\langle|\tilde{F}(f)|^2\rangle}{(2\pi\gamma)^2 f^2}. \tag{2}$$

As $F(t)$ is a white noise term $\langle|\tilde{F}(f)|^2\rangle$ is a constant and hence $\langle|\tilde{x}(f)|^2\rangle \propto \frac{1}{f^2}$.

However, this relation is only valid in purely viscous fluids. If particles are diffusing in an environment where their motion is restricted by, for example, hard obstacles or semi-flexible polymers [15], the equation of motion changes to

$$m\ddot{x}(t) = -\gamma\dot{x}(t) + F(t) + F_A(t), \tag{3}$$

where $F_A(t)$ describes the additional interactions of the particles. In this situation, and in a limited frequency range, the power spectrum follows

$$\langle|\tilde{x}(f)|^2\rangle \propto \frac{1}{f^{(1+\alpha)}}. \tag{4}$$

If the exponent α is smaller than 1, the motion of the particle is restricted, and the particle undergoes subdiffusion. Subdiffusion is typical for particles moving in viscoelastic media. If $\alpha > 1$ the motion is superdiffusive. Superdiffusive behavior can be induced, e.g., by convective processes in the medium or by active transportation within the cell. For $\alpha = 1$ the particle performs normal Brownian motion [25].

The optical tweezers exert a harmonic force on the trapped particle, and in purely viscous media the resulting positional power spectrum is well fitted by a Lorentzian function. The corner frequency of the Lorentzian denotes the frequency below which a trapped particle feels the presence of the trap and above which the particle is performing Brownian motion with amplitudes small enough that the restriction by the trap is not felt by the particle. A similarly simple expression for the power spectrum of a trapped particle in a viscoelastic medium does not exist. Yet, the influence of the trap will in a similar manner be dominant below the corner frequency. In our experiments the laser power was very low, hence, the corner frequency was correspondingly low (below 100 Hz). We avoided the necessity to account for the effect of the optical trap by choosing to fit the theoretical expression in equation (4) to the data in a frequency regime well above the corner frequency.

To find α, equation (4) was fitted to the power spectra that are calculated from positional time series recorded by the photodiode. We performed the analysis using a custom-made Matlab program, a modification of the one presented in [26], where we also accounted for the significant filtering caused by the quadrant photodiode [27] and the amplifier by including two first-order filters at 50 and 80 kHz [28]. For the analysis we used the frequency interval between 350 Hz and 6000 Hz in order to omit high-frequency noise from the electronics and low-frequency noise from the cooling system of the camera and intracellular convective processes.

3. Results and discussion

3.1. Division of data into different stages of the cell cycle

For every single granule we recorded both a fluorescent picture and a bright field picture. These images allowed us to determine the position of the granule in the cell with respect to the nucleus and the outer membrane and to determine the cell's stage in the cell cycle. Figure 1 shows fluorescent images of various cells combined with schematic drawings of the cell at that particular stage. As only the membrane systems (and not, e.g., microtubules) were fluorescently marked, we had to group the cells into stages that could be defined on the basis of the appearance of their membranes. Hence, it was not possible for us to distinguish interphase cells (stage 0 in figure 1) from prophase cells (stage 1 in figure 1). However, as the cells spend significantly more time in interphase than in prophase, the results from what we termed 'stage 0/1' almost all stem from interphase cells. Also, prophase cells should be more elongated than interphase cells, and as we saw no significant change in length of the cells termed 'stage 0/1', we have further reason to believe that almost all of the measurements from cells in this stage reflect the properties of interphase cells.

Our 'stage 2' refers to early anaphase where the two daughter nuclei begin to separate. 'Stage 3' is late anaphase (or early telophase), i.e. when the two daughter nuclei have reached the ends of the cell. 'Stage 4' is when there is a clear new cell wall separating the two daughter cells, but where the cells have not yet divided and the two daughter nuclei are not at the center of the new cells (early cytokinesis). 'Stage 5' is late cytokinesis where the cells have clearly separated, with the nuclei in the center of the newly formed cells.

3.2. Rheological exponents

In a laser tracking experiment we obtained a time series of a typical granule as, e.g., shown in the inset of figure 3(*a*). The histogram shown in figure 3(*a*) displays the position histogram of a 3 s long time series. The units are in Volts and can be directly translated to distance, but this is not necessary for the analysis presented here. Overall, the particle positions nicely follow a Gaussian distribution, although the time series of positions also show jumps and irregularities between different positions. In (*b*) we show a comparison of the power spectra for a granule in the trap (red), the background noise inside a cell (blue) and the background noise in the aqueous environment outside a cell (black). The signal recorded with a granule in the laser trap is orders of magnitude larger than the two other signals, and consequently intracellular noise cannot be mistaken for a signal stemming from a granule. Also, bright field pictures with focus identical to that of the optical trap ensure that indeed only one granule is in the trap. The reason

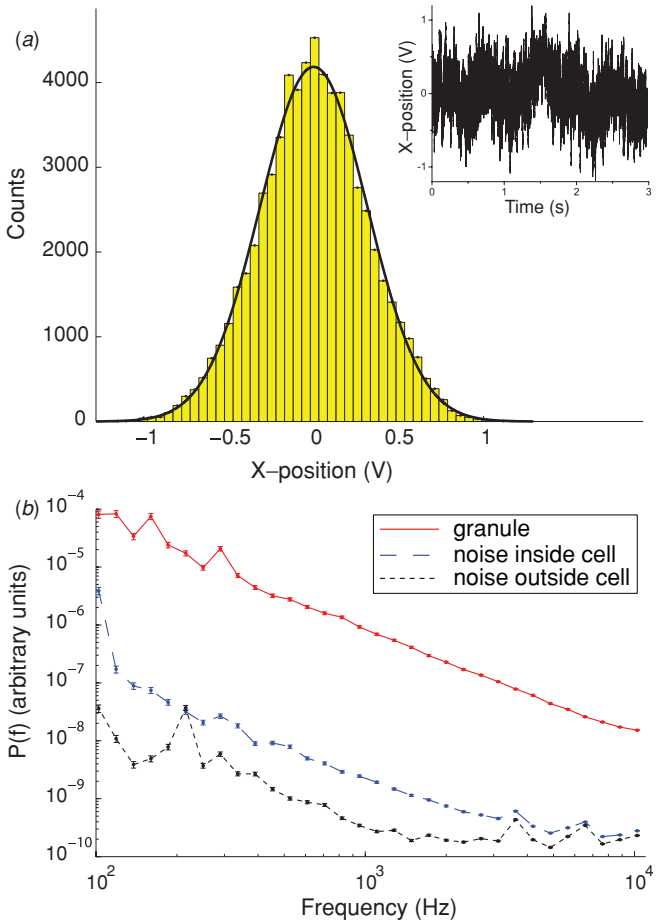

Figure 3. (*a*) Histogram and time series (inset) of granule positions in the laser trap. (*b*) Power spectra for a granule in the trap (red solid line), the background noise inside a cell (blue dashed line) and the background noise outside a cell (black dotted line).

why the power spectral background signal from within the cell is larger than outside the cell is probably that intracellular particles smaller than the resolution of the microscope get trapped by the focused laser and give rise to a small signal.

Table 1. The values of the subdiffusive exponent, α, from five stages of the cell cycle, the standard error in the mean of the exponent, and the number of granules investigated, n. Often several granules were investigated from a particular cell. Stage 0/1 is predominantly from cells in interphase, stages 2–5 are during cell division.

α_{stage}	Value	SEM	n
$\alpha_{0/1}$	0.8146	0.0068	151
α_2	0.8413	0.0049	166
α_3	0.8340	0.0054	200
α_4	0.8446	0.0066	145
α_5	0.8490	0.0097	81

In the data analysis we fitted equation (4) to the positional power spectrum in the frequency range [350 Hz, 6000 Hz]. An example of such a fit is shown in figure 4. In (*a*) the fitting region is shown by filled symbols, (*b*) shows the data divided by the fit, the dotted lines denote one standard deviation and 2/3 of the data/fit fall within the two dotted lines. Furthermore, the quality of the fit is demonstrated by the even distribution of data points as a function of frequency. Values for the exponent, α, were extracted from fits with a support larger than 1 per mille.

The distributions of the values found for the exponents, α, are shown in figure 5 for each of the 5 stages. Overlaid is a plot of a Gaussian function with the same mean and width. Table 1 summarizes the mean values for the subdiffusive exponent found for each stage, the standard error on the mean, and the number of data points in each stage. In a previous investigation of granules in interphase cells, we performed a series of control experiments [13]. For example, we found the rheological exponent of a lipid granulus dissolved in water to be 1.004 ± 0.0003, as it should be for a particle performing Brownian motion in a purely viscous medium.

3.3. Change of rheological exponents during cell cycle

In order to evaluate whether the values found for the exponents from the different stages differed, we performed a series of Student's t-tests. The results from testing each stage against

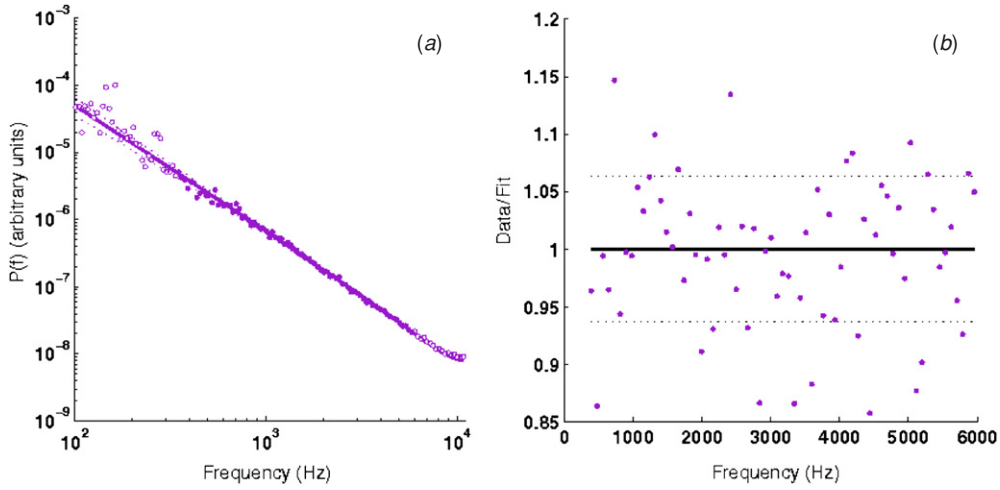

Figure 4. (*a*) Fit of the power spectrum in the interval [350 Hz, 6000 Hz]. (*b*) Data/fit for the fit shown in (*a*).

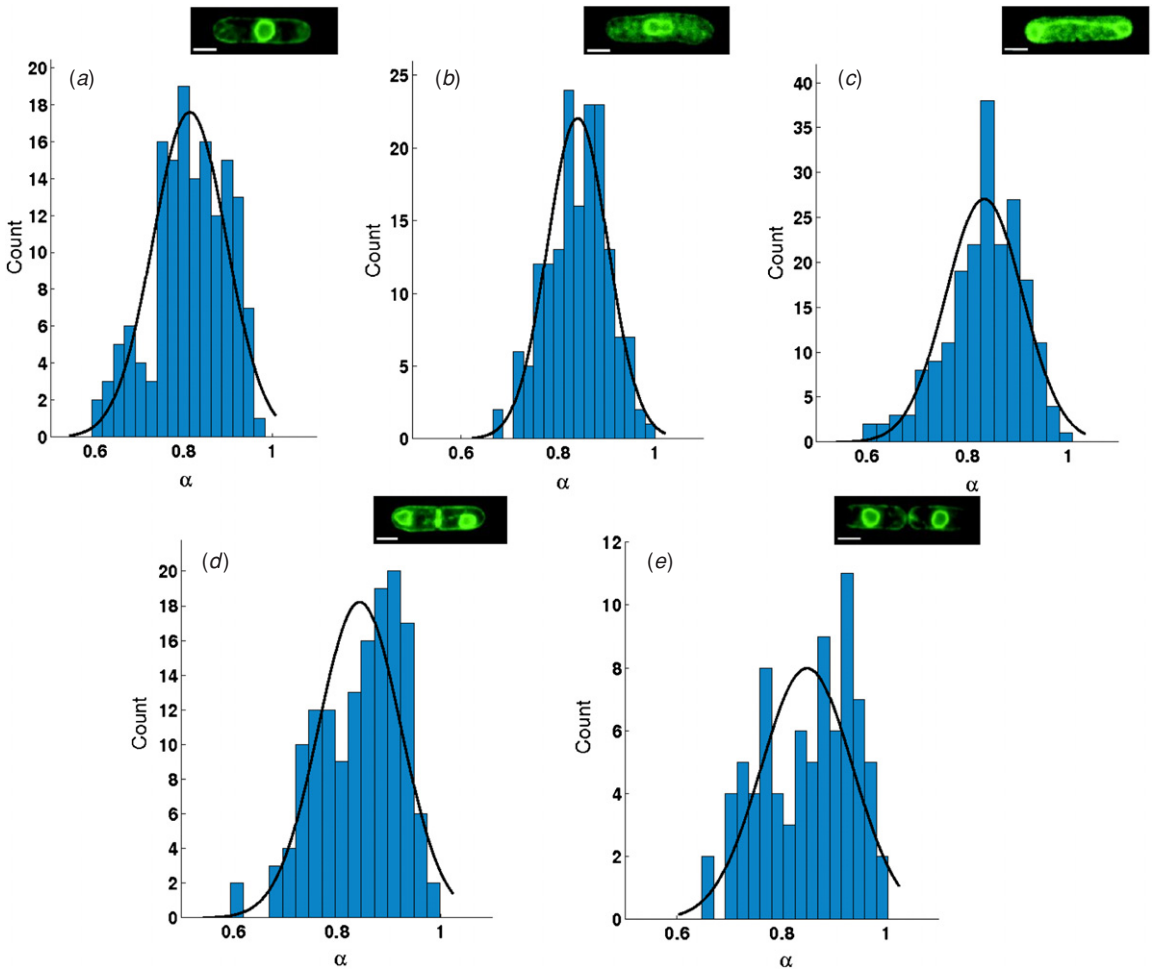

Figure 5. Histograms showing the values found for the subdiffusive exponents, α, for each of the five stages. (*a*) stage 0/1, (*b*) stage 2, (*c*) stage 3, (*d*) stage 4, (e) stage 5. Scale bar in pictures is 5 μm.

Table 2. The *p*-values calculated with a Student's t-test giving the probability that the observed differences in subdiffusive exponents between the different stages of cell division is accidental.

Stage	2	3	4	5
0/1	0.0013	0.0238	0.0017	0.0036
2	–	0.3228	0.6844	0.4314
3	–	–	0.2114	0.1547
4	–	–	–	0.7019

the four other stages are summarized in table 2. The *p*-value given for each set of two stages gives the probability that the observed difference between the two stages is accidental. Often, a *p*-value of 0.05 is used as a threshold criterion between the two hypotheses. In other words, a low *p*-value supports the hypothesis that the two stages have significantly different viscoelastic properties, a high value supports the hypothesis that the viscoelastic properties of the two stages are the same. From the values given in table 2 it is clear that the exponents obtained from cells in 'stage 0/1' are significantly different from the exponents in all other stages. Similarly, the exponents from stages 2, 3, 4, and 5 (all during cell division) appear similar. A graphic illustration of this is shown in figure 6 which displays the value of α with error bars at each stage.

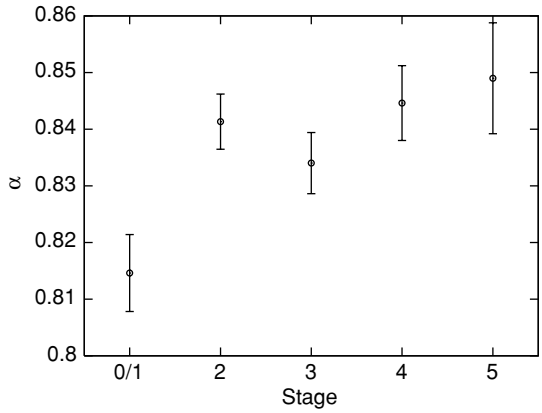

Figure 6. Value of α as a function of cell division stage. Error bars show the standard error on the mean.

The conclusion is thus that the viscoelastic properties of the cell cytoplasm during interphase, as measured by the subdiffusive exponent α, are significantly different from the viscoelastic properties during mitosis and cytokinesis. With our resolution, we are not able to detect any changes of the viscoelastic properties during the different stages of mitosis and cytokinesis.

In the previous study of the diffusion of lipid granules in interphase cells, at short timescales the granules were found to perform subdiffusive motion [13], in accordance with the present results. However, the obtained exponent was somewhat smaller ($\alpha = 0.737 \pm 0.003$ [13]) than the exponent obtained in the present study ($\alpha = 0.815 \pm 0.007$). One possible explanation for the discrepancy between the two results could be that the frequency fitting interval from the positional power spectrum in [13] was [200 Hz, 2 kHz], which is a narrower interval than the frequency used in the present study ([350 Hz, 6 kHz]) and also starting at lower frequencies. The higher minimum frequency in the fitting interval chosen in the present study is important, because the restoring effect of the optical trap is present in the part of the frequency spectrum which is lower than or around the corner frequency. In other words, it is important to start the frequency interval for fitting well above the corner frequency.

In the previous study [13] the distinction between whether the cells were in interphase or in mitosis (or cytokinesis) was done in exactly the same manner as in the present study. Hence, the cells in prophase were also counted (as a minority) of the interphase cells. The fact that we, with the current strain used, were not able to distinguish interphase from prophase cells might increase the observed value of α in comparison to a sample which only originated from interphase cells. However, as we expect the fraction of prophase cells to be minor in comparison to the interphase cells in 'stage 0/1', this effect is small.

During interphase long bundles of microtubules expand the cytoplasm of the cell and constitute an important part of the cytoskeleton. During mitosis these bundles depolymerize and are less abundantly present in the cytoplasm. Our results show that the cytoplasm is more elastic during interphase than during mitosis. This fact correlates well with the presence (or absence) of long bundled microtubules during interphase (or mitosis) and we hypothesize that the microtubules are responsible for part of the elastic behavior of the cell cytoplasm. Also, the microtubules could serve as obstacles or confine the motion of the granules. In the previous study of lipid granules in interphase cells [13], the cells were treated with Cytochalasin D, a drug known to disrupt the intracellular actin filaments. This chemical disruption of actin gave rise to a smaller, but still significant, increase of the rheological exponent. Hence, we know that disrupting part of the cytoskeleton in *S. pombe* yeast cells gives rise to changes in the rheological exponent that are on the same order as the observed difference between interphase and mitotic cells. This renders it likely that the observed difference in rheological exponents between interphase and mitotic cells could be due to the depolymerizing of microtubules during mitosis. As the cytoplasm is very dense and contains several other viscoelastic structures, the change in rheological exponent connected with disruption of microtubules does not need to be very large.

In a recent microrheological study of the cytoplasm of *Amoeba proteus* [8] it was found that endogenous particles at short timescales exhibited subdiffusive motion characterized by a rheological scaling exponent of 3/4. This value is somewhat smaller than the values we found for the *S. pombe* cells, but as the error bars are unknown, the numbers could coincide. Anomalous subdiffusion was also observed for proteins in the cytoplasm of HeLa cells [29], where it was proposed to use anomalous subdiffusion as a measure of the cytoplasmic crowding in living cells. The authors used FCS to monitor diffusion of proteins of various sizes and in two out of three cases they found that the rheological exponent was larger for interphase cells than for mitotic cells. Only for the middle sized protein they observed the same behavior as we report, namely that the rheological exponent was larger in interphase than during mitosis. However, it might not be valid to compare the two experiments, because diffusion of proteins which are foldable, flexible polymers is considerably more complicated than diffusion of the spherical hard lipid granules used in the present study. Also, the cell types are very different.

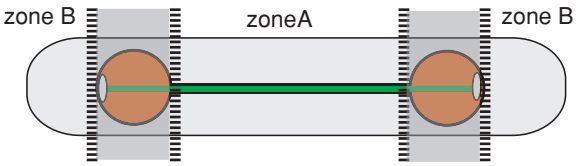

Figure 7. Drawing of the division of the cell cytoplasm during anaphase into zones. Zone A is between the two moving daughter nuclei, zone B is between the nuclei and the ends of the cell. The regions adjacent to the daughter nuclei were not analyzed.

A couple of studies have addressed the motility of proteins inside *E. coli* bacteria [30, 31]: the diffusion of GFP was found to be dependent, e.g., on GFP expression level [30] and in general, the viscoelasticity was found to vary. By following the motion of fluorescently labeled mRNA molecules, it was found that their motion is subdiffusive with a rheological exponent which is independent of disruption of the cytoskeletal elements MreB and FtsZ [31]. The cytoskeletons of a eucaryotic cell (such as *S. pombe*) and a procaryotic cell (such as *E. coli*) are entirely different, e.g., the procaryotes do not have polymerized microtubules (or anything similar) spanning the entire cytoplasm. Hence, the two systems are difficult to compare. Also, in two mentioned studies of *E. coli* there was no track of the cell divisional state of the bacteria investigated, which is the key issue in the present study of *S. pombe* yeast cells.

3.4. Dependence of rheological exponents on granule position

In order to investigate whether the viscoelastic landscape of the cytoplasm had local variations, we divided the cells into different zones and compared the diffusion of the lipid granules in the different zones. One division was done as shown in figure 7 where cells in anaphase (stage 2 and 3) were divided into a 'zone A' between the two daughter nuclei and a 'zone B' between the two daughter nuclei and the edges of the cell. The region just adjacent to the two daughter nuclei (dark gray in figure 7) was not analyzed. The reasoning behind this division into zones was a speculation of whether it could be advantageous for the cell if the cytoplasm between the two daughter nuclei were more elastic (to prevent

back-flow of the daughter nuclei) than the region outside the daughter nuclei. The outcome of the analysis was that $\alpha_A = 0.8331 \pm 0.0060$ (average $\pm$ SEM), $n = 107$, and $\alpha_B = 0.8374 \pm 0.0051, n = 150$. A Student's t-test shows that the probability that the observed difference is accidental is 0.58. Hence, with our resolution, we see no difference between these two zones. In addition, we tried to divide the interphase cells into zones dependent on the distance to the nuclei. Also in this case, our analysis was not able to detect any significant difference in viscoelastic properties as a function of localization of the granules with respect to the nucleus.

These observations support the overall hypothesis that for *S. pombe* yeast cells the presence or absence of polymerized microtubules (expanding the entire cytoplasm) is important for the viscoelastic properties. For other organisms it might be different; in the study of *Amoeba proteus* the rheological exponent was 0.78 and 0.74 in the front and back regions, respectively [8].

4. Summary and outlook

We investigated the diffusion of naturally occurring lipid granules inside living *S. pombe* yeast cells at different stages of the cell cycle. The diffusion of the lipid granules was tracked nearly non-invasively by optical tweezers with millisecond and nanometer resolution. We divided the cell cycle into interphase and mitosis, and further divided mitosis into four stages. The positional power spectrum, or similarly, the mean squared displacement, of each lipid granule was well described by a rheological exponent. The value of the exponent determined from cells in interphase was found to be significantly smaller than the value from cells in any stage of mitosis. During mitosis we could not detect any change in the rheological exponent. Also, we addressed the issue of whether the rheological exponent would depend on the localization of the granulus. The cell was divided into different zones, e.g., by comparing the regions between and outside the two daughter nuclei, or by comparing zones with different distances to the cell nucleus. However, none of those investigations showed any dependence of the rheological exponent on subcellular localization. Our results show that the cytoplasm is more elastic, less viscous, during interphase than during mitosis. This correlates well with the fact that microtubules, an elastic part of the cytoskeleton, are less abundantly present during mitosis than during interphase.

To address this point more carefully, in future experiments strains with fluorescent microtubules should be invoked. It is our hope that such genetic modifications will not affect cell viability. Measuring diffusional properties of granules adjacent to microtubules will allow a possible verification of the above hypothesis of whether the presence of microtubules is crucial for the elasticity of the cytoplasm. Also, it will allow for a clear distinction between interphase and prophase cells.

In the experiments the rheological scaling exponent was found from the slope of the positional power spectrum. The ergodicity theorem states that, if the time window and spatial environment are sufficiently large, the mean squared displacement found by an average over an ensemble should be consistent with the value found from a time average of the mean squared displacement of a single trajectory. Interestingly, a recent publication [32] shows that in typical cellular probe tracking experiments, this might not be the case: the cell only has a finite size and the time window is typically not large enough to permit a reliable time average of the trace of a single particle. In the present study, we chose to only focus on the rheological scaling exponents found by ensemble averaging, and future experiments will address the very interesting issue of possible ergodicity breaking in subdiffusive motion of lipid granules in living yeast cells.

Acknowledgments

We thank Genevieve Thon for stimulating discussions and for providing the *S. pombe* cells. This work was funded by the Villum Kann Rasmussens Foundation through BioNET, an Excellence grant from University of Copenhagen, and the German Academy of Sciences Leopoldina through grant BMBF-LPD 9901/8-164.

Glossary

Schizosaccharomyces pombe. Fission yeast cells (*Schizosaccharomyces Pombe, S. pombe)* are rod-shaped eucaryotic cells that are widely used by biologists for cell cycle studies, because genetic modifications are easily amenable. This makes *S. pombe* a good model for studying the effects of genetic modifications on cell division. Other advantages of *S. pombe* cells are that their cell division process is similar to the one in human cells and the simplicity of their cytoskeleton, whose organization and composition is well understood.

Mitotic cell division. The first step of cell division is always the replication of the chromosomes. In mitotic cell division, an organized network of microtubules forms, the mitotic spindle. During *mitosis*, the mitotic spindle separates the replicated chromatids from the disintegrated cell nucleus and provides the mechanical framework for the separation of the daughter chromatids. Mitosis is an essential prerequisite for the formation of the two daughter cells in the later *cytokinesis*.

Mitosis proceeds in five distinct phases: the first phase is the *prophase*, where the microtubules arrange in the form of a spindle. In the *pro-metaphase* the nuclear envelope breaks down and the chromosomes can attach to spindle microtubules via kinetochores. In the *metaphase* the active movement of the microtubules aligns the chromatids at the equator of the spindle. At this stage the chromosomes are held under considerable tension by microtubules that are attached to opposite poles of the spindle. In the *anaphase* the chromatids form two daughter chromosomes, which are pulled toward the two spindle poles where they arrive in the *telophase*.

During cytokinesis the mother cell topologically splits up into the two daughter cells which become independent entities.

Optical tweezers. Optical tweezers are a device that allows for manipulation of nano- and microscopic particles by a focused laser beam. In biological experiments, typically infrared lasers are used, because they are nearly non-invasive to biological systems provided that the correct wavelength and low laser powers are used [22]. Importantly, optical tweezers are the only nanotool which is able to reach inside a living organism and manipulate organelles without disrupting the membrane surrounding the organism. With optical tweezers, forces can be measured in the sub-piconewton to piconewton regime and distances down to fractions of nanometers.

Anomalous diffusion. In Brownian motion, the mean-squared displacement of the diffusing particle is proportional to time, i.e. $\langle \Delta x(t)^2 \rangle \propto t$. If diffusion is hindered, e.g., by collisions with obstacles, or if active processes push the particle forward, the relation between the mean-squared-displacement changes to $\langle \Delta x(t)^2 \rangle \propto t^{\alpha}$, where $\alpha < 1$ for restricted diffusion (subdiffusion) and $\alpha > 1$ when active processes enhance particle motion (superdiffusion).

References

[1] Scholey J M, Brust-Mascher I and Mogilner A 2003 Cell division *Nature* **422** 746–52

[2] Hayles J and Nurse P 2001 A journey into space *Nat. Rev. Mol. Cell. Biol.* **2** 647–56

[3] Forsburg S L and Nurse P 1991 Cell cycle regulation in the yeasts *saccharomyces cerevisiae* and *schizosaccharomyces pombe Ann. Rev. Cell Biol.* **7** 227–56

[4] Chang F and Nurse P 1996 How fission yeast fission in the middle *Cell* **84** 191–4

[5] Mason T G and Weitz D A 1995 Optical measurements of frequency-dependent linear viscoelastic moduli of complex fluids *Phys. Rev. Lett.* **74** 1250–3

[6] Guigas G, Kalla C and Weiss M 2007 Probing the nanoscale viscoelasticity of intracellular fluids in living cells *Biophys. J.* **93** 316–23

[7] Tseng Y, Kole T P and Wirtz D 2002 Micromechanical mapping of live cells by multiple-particle-tracking microrheology *Biophys. J.* **83** 3162–76

[8] Rogers S S, Waigh T A and Lu J R 2008 Intracellular microrheology of motile amoeba proteus *Biophys. J.* **94** 3313–22

[9] Gardel M L, Valentine M T, Crocker J C, Bausch A R and Weitz D A 2003 Microrheology of entangled f-actin solutions *Phys. Rev. Lett.* **91** 158302

[10] Helfer E, Harlepp S, Bourdieu L, Robert J, MacKintosh F C and Chatenay D 2000 Microrheology of biopolymer–membrane complexes *Phys. Rev. Lett.* **85** 457

[11] Helfer E, Harlepp S, Bourdieu L, Robert J, MacKintosh F C and Chatenay D 2001 Viscoelastic properties of actin-coated membranes *Phys. Rev.* E **63** 021904

[12] Yamada S, Wirtz D and Kuo S C 2000 Mechanics of living cells measured by laser tracking microrheology *Biophys. J.* **78** 1736–47

[13] Tolic-Nørrelykke I, Munteanu E-L, Thon G, Oddershede L and Berg-Sørensen K 2004 Anomalous diffusion in living yeast cells *Phys. Rev. Lett.* **93** 078102

[14] Amblard F, Maggs A C, Yurke B, Pargellis A N and Leibler S 1996 Subdiffusion and anomalous local viscoelasticity in actin networks *Phys. Rev. Lett.* **77** 4470

[15] Schnurr B, Gittes F, MacKintosh F C and Schmidt C F 1997 Determining microscopic viscoelasticity in flexible and semiflexible polymer networks from thermal fluctuations *Macromolecules* **30** 7781–92

[16] Claessens M M A E, Tharmann R, Kroy K and Bausch A R 2006 Microstructure and viscoelasticity of confined semiflexible polymer networks *Nat. Phys.* **2** 186–9 (1745-2473 10.1038/nphys241 10.1038/nphys241)

[17] Mizuno D, Tardin C, Schmidt C F and MacKintosh F C 2007 Nonequilibrium mechanics of active cytoskeletal networks *Science* **315** 370–3

[18] Munteanu E-L, Olsen A L, Tolic-Nørrelykke I, Flyvbjerg H, Oddershede L and Berg-Sørensen K 2006 Quantitative studies of subdiffusion in living cells and actin networks *Biophys. Rev. Lett.* **1** 411–21

[19] Caspi A, Granek R and Elbaum M 2000 Enhanced diffusion in active intracellular transport *Phys. Rev. Lett.* **85** 5655

[20] Ding D Q, Tomita Y, Yamamoto A, Chikashige Y, Haraguchi T and Hiraoka Y 2000 Large-scale screening of intracellular protein localization in living fission yeast cells by the use of a GFP-fusion genomic DNA library *Genes to Cells* **5** 169–90

[21] Robinow C F and Hyams J S 1989 General cytology of fission yeast *Molecular Biology of the Fission Yeast* (New York: Academic) pp 273–330

[22] Rasmussen M B, Oddershede L B and Siegumfeldt H 2008 Optical tweezers cause physiological damage to *e. coli* and listeria bacteria *Appl. Environ. Microbiol.* **74** 2441–6

[23] Mirsaidov U, Timp W, Timp K, Mir M, Matsudaira P and Timp G 2008 Optimal optical trap for bacterial viability *Phys. Rev.* E **78** 021910–1

[24] Peterman E J G, Gittes F and Schmidt C F 2003 Laser-induced heating in optical traps *Biophys. J.* **84** 1308–16

[25] Metzler R and Klafter J 2000 The random walk's guide to anomalous diffusion: a fractional dynamics approach *Phys. Rep.* **339** 1–77

[26] Hansen P M, Tolic-Nørrelykke I M, Flyvbjerg H and Berg-Sørensen K 2006 Tweezercalib 2.1: Faster version of matlab package for precise calibration of optical tweezers *Comput. Phys. Commun.* **175** 572–3

[27] Berg-Sørensen K, Oddershede L, Florin E-L and Flyvbjerg H 2003 Unintended filtering in typical photo-diode detection system for optical tweezers *J. Appl. Phys.* **93** 3167–76

[28] Berg-Sørensen K and Flyvbjerg H 2004 Power spectrum analysis for optical tweezers *Rev. Sci. Instrum.* **75** 594–612

[29] Weiss M, Elsner M, Kartberg F and Nilsson T 2004 Anomalous subdiffusion is a measure for cytoplasmic crowding in living cells *Biophys. J.* **87** 3518–24

[30] Elowitz M B, Surette M G, Wolf P-E, Stock J B and Leibler S 1999 Protein mobility in the cytoplasm of *escherichia coli J. Bacteriol.* **181** 197–203

[31] Golding I and Cox E C 2006 Physical nature of bacterial cytoplasm *Phys. Rev. Lett.* **96** 098102–4

[32] He Y, Burov S, Metzler M and Barkai E 2008 Random time-scale invariant diffusion and transport coefficients *Phys. Rev. Lett.* **101** 058101